Available online at www.sciencedirect.com

Energy Procedia 00 (2013) 000–000

=SAND2013-5257C=
Energy Procedia

www.elsevier.com/locate/procedia

SolarPACES 2013X

Annual average efficiency of a solar-thermochemical reactor

I. Ermanoski[a]*, N. Siegel[b]

[a]*Materials, Devices & Energy Technologies Dept. Sandia National Laboratories; PO Box 5800, MS 1415, Albuquerque, NM, 87185-1415,USA*
[b]*Mechanical Engineering Department. Bucknell University, Lewisburg, PA, 17837, USA*

Abstract

We report on results regarding the annual average efficiency of a recuperating packed particle bed for solar-thermochemical hydrogen production via a two-step metal oxide cycle, using advanced numerical models. The key findings are that reactor efficiency is substantially flat as a function of direct normal irradiance, leading to an annual average efficiency almost equal to the design-point efficiency, and that ample high quality waste heat is available to make standalone operation feasible, including feedstock production. This conclusion has far-reaching implications for solar-thermochemical hydrogen and fuel production in general.

Keywords: Solar fuels; thermochemical; hydrogen;

1. Introduction and approach

Solar-thermochemical fuel production has the potential to deliver exceptional solar-to-fuel efficiencies, and dramatically change the world's renewable energy posture. The most promising approach, two-step cycles, is nominally quite straightforward: a working material (oxide) is partially reduced at a high temperature, then cooled and exposed to steam, for example, to be reoxidized and to produce hydrogen. The high temperature requirement for

* Corresponding author. Tel.: +1-505-284-0740; fax:+1-505-844-5470.
E-mail address: iermano@sandia.gov

the reduction step of the cycle naturally poses a question regarding the efficiency, even feasibility, of such a process under conditions of decreased direct normal irradiance (DNI), whether owing to cloud cover or low solar elevation.

To answer this question, we analyze the operation of the reactor described in detail in [1], illustrated in Fig. 1a, which consists of three main parts: A *thermal reduction chamber*, a *recuperator* (solid-solid heat exchanger), and a *fuel production chamber*. During operation, concentrated solar radiation directly heats and thermally reduces the reactive particles in the thermal reduction chamber (at temperature T_{TR} and pressure p_{TR}). They are then moved through the recuperator (entering at the hot inlet) and then into the fuel production chamber, where they are exposed to steam (at temperature T_{FP}), producing H_2. The reoxidized particles are the brought to the (cold) inlet of the recuperator and moved toward the reduction chamber in a countercurrent flow arrangement with respect to the reduced particles moving toward the fuel production chamber. This maximizes heat recovery between the two reactive material flows.

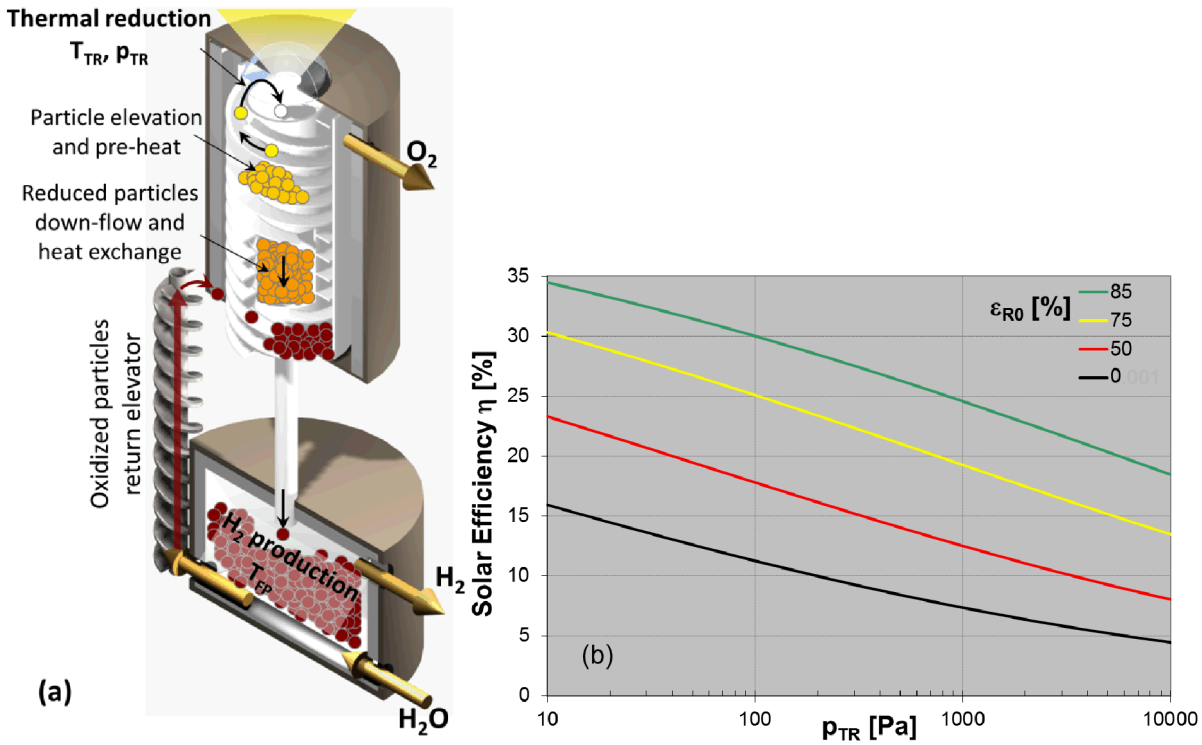

Figure 1. (a) Schematic drawing of the moving packed particle bed reactor. The packed bed of particles fills the entire reactor, but is only shown selectively, to preserve the clarity of the schematics (b) Solar efficiency as function of p_{O2} for several values of ε_{R0}, at DNI=1 kW/m^2.

The basis for the *annual average efficiency*, η_{AA}, is the *solar-to-H_2 efficiency* (η), also referred to as *solar efficiency*:

$$\eta = \frac{\dot{n}_{H_2} HHV_{H_2}}{P_S} \qquad (1).$$

The efficiency assumptions and calculations are identical to those in [1], where a detailed description is given. We briefly summarize these details here, noting that the thermodynamic parameters for ceria used in the calculations are based on experiments by Panlener et al. [2]: The molar rate of H_2 production, $\dot{n}_{H_2}$ in Eq. 1 is:

$$\dot{n}_{H_2} = \frac{P_{TH}}{Q} \quad (2).$$

Here P_{TH} is the solar heat power, available after losses to reflection, window transmission, aperture intercept, and thermal re-radiation (P_{rad}) through the aperture:

$$P_{TH} = r_{12} * r_d * t_W * A * P_S - P_{rad} \quad (3),$$

and Q is the heat required for the production of 1 mol H_2:

$$Q = Q_{TR} + Q_{SH} + Q_{AUX} \quad (4).$$

Here $Q_{TR}=\Delta_r H(CeO_2)$ is the heat required for the thermal reduction of the oxide (per mole H_2).
The energy required for heating the oxide from T_{FP} to T_{TR} is:

$$Q_{SH} = \frac{C_{OX}}{\delta}\left(T_{TR} - T_{FP}\right)\left(1 - \varepsilon_R\right) \quad (5),$$

where ε_R is the recuperator effectiveness, and $C_{OX}\approx 80$ J/mol K is the molar heat capacity of CeO_2.[3] Finally, Q_{AUX} encompasses the heat equivalent of all other reactor needs:

$$Q_{AUX} = Q_{H_2O} + Q_{pump} + Q_{mech} - Q_{MOX} - Q_{SH} - Q_{O_2} \quad (6) \quad .$$

Here Q_{H2O} is the heat needed for steam generation and heating. The heat equivalent of the pumping of products (from both chambers) and mechanical work for particle moving are Q_{pump} and Q_{mech}, respectively The negative terms represent the waste heat available from the product gasses, mainly the H_2O-H_2 mix that can be used to provide mechanical work. The heat released in the reoxidation step is $Q_{MOX}=\Delta_r H-\Delta H_c^{\ 0}{}_{H2}$, Q_{SH} is the sensible heat of the oxide that must be removed before reoxidation (equal to that in Eq. 5), and Q_{O2} is the heat in the oxygen output stream. When Q_{AUX} is negative (i.e. when there is unneeded waste heat), it is excluded from the calculations, as waste heat from the product gasses cannot be used to contribute to either the heating or the thermal reduction of CeO_2.

Only solar primary energy is used for the entire operation of the reactor and all reactions end in their thermodynamic equilibrium states. Shading and blocking were not included since the calculation is for one parabolic dish concentrator. The nomenclature and parameters used for these design-point calculations are summarized in Table 1, and Fig. 1b shows the calculated values of η.

Table 1. Nomenclature, with values and design-point values, where applicable.

Nomenclature

Symbol	Description	Design point value
DNI	direct normal irradiance	1 kW/m^2
T_{TR}	thermal reduction temperature	1500°C
T_{FP}	water splitting temperature	1100°C
p_{TR}	thermal reduction pressure	100 Pa
η	solar-to-hydrogen efficiency	
$\dot{n}_{H_2}$	H_2 production rate [mol/s]	
HHV_{H2}	hydrogen higher heating value	286 kJ/mol
P_S	solar power incident on primary concentrator [W]	
P_{TH}	solar heat available after collection losses [W]	
Q	heat required for the production of 1 mol H_2 [J/mol H_2]	
P_{TH}	solar heat available after collection losses [W]	
r_{12}	combined mirror reflectivity	0.925
r_d	dirt factor	0.95

t_W	window transmission	0.95
A	solar intercept	0.95
P_{rad}	blackbody re-radiation through aperture [W]	
Q_{TR}	heat required for the oxide reduction, per mole H_2 [J/mol H_2]	
Q_{SH}	sensible heat required for oxide heating, per mole H_2 [J/mol H_2]	
Q_{AUX}	heat equivalent of auxiliary work per mole H_2 [J/mol H_2]	
C_{OX}	cerium oxide molar heat capacity [J/mol K]	80000
δ	extent of oxide reduction	
ε_R,ε_{R0}	recuperator effectiveness	
Q_{H2O}	heat required for steam generation and heating per mole H_2 [J/mol H_2]	
Q_{pump}	heat equivalent of pump work per mole H_2 [J/mol H_2]	
Q_{mech}	heat equivalent of mechanical work per mole H_2 [J/mol H_2]	
Q_{MOX}	heat released in the H_2 production step (reoxidation) per mole H_2 [J/mol H_2]	
Q_{O2}	waste heat in the O_2 output stream per mole H_2 [J/mol H_2]	
$\Delta_r H$	enthalpy of reduction	
$\Delta H_c^{\ 0}{}_{H2}$	standard heat of combustion for hydrogen (=HHV_{H2})	
η_{AA}	annual average solar efficiency	

2. Results and discussion

To evaluate low-DNI solar efficiency, η(DNI), we first choose an additional design point value: $p_{TR,0}$=100 Pa. This design-point pressure is chosen with consideration of pumping speed limits [1], rather than simply opting for the highest design-point efficiency by choosing the lowest p_{TR} value. At the design point $\eta=\eta_0$.

A simple, first-order approach for evaluating η(DNI) is then to only decrease DNI in the input parameters. This makes radiation losses through the aperture a relatively higher fraction of the overall losses (Eq. 3), decreasing efficiency with DNI decrease, as shown in Fig. 2. From the consistently lower η(DNI) at low DNI, it follows that the annual average solar efficiency, η_{AA}, is lower than η_0. There are, however, two more important factors to consider before correctly evaluating η_{AA}.

Firstly, as DNI decreases, so does the rate of oxide flow through the reactor, simply because less power is available for the thermal reduction step of the cycle and oxide flow must be adjusted accordingly to maintain T_{TR}. This decreased oxide flow increases ε_R by virtue of the increase in the time the oxide spends in the recuperator, effectively making ε_R a function of DNI. At the design point, $\varepsilon_{R0}=\varepsilon_R(1\ kW/m^2)$. To account for this, we assume that the recuperator behaves ideally – i.e. its effectiveness exponentially approaches unity as flow approaches zero. The limits of this approximation are discussed below.

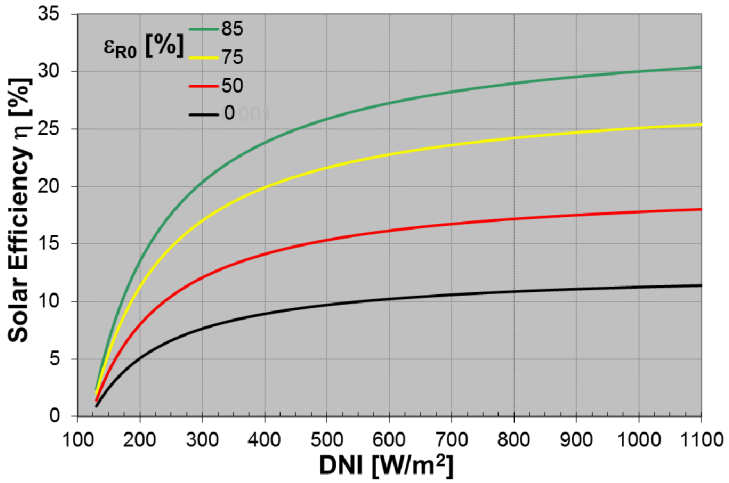

Figure 2. First order calculation for η(DNI) away from the design point for several values of ε_{R0}.

Secondly, the O_2 production rate in the thermal reduction chamber also decreases with DNI decrease. At a given nominal pumping speed this makes p_{TR} a function of DNI, as well. This follows the inverse relationship between volume (of evolved oxygen) and pressure, leading to substantial p_{TR} decrease at decreased DNI. It should be noted here that even though pumping work increases with p_{TR} decrease, overall efficiency increases. This is the main reason to assume this mode of operation, as opposed to decreasing pumping speed with DNI decrease, so as to maintain constant p_{TR}. In this context, we note here again that oxygen volumetric flow and related pump size is the main limitation to the lowest p_{TR} that can be achieved in practice, not pumping work considerations.

The dependence of ε_R and p_{TR} on DNI makes the η(DNI) calculation iterative, as it is mediated by the oxide flow which, in turn, depends on DNI for a given nominal power of the reactor. The results of the converged iterations are shown in Fig. 3 and are substantially different from the simple model results. The most prominent, if not entirely unexpected feature of the η(DNI) curves, is an actual efficiency *increase* at low DNI, up to the point where radiation through the aperture becomes a dominant contribution in the reactor energy balance.

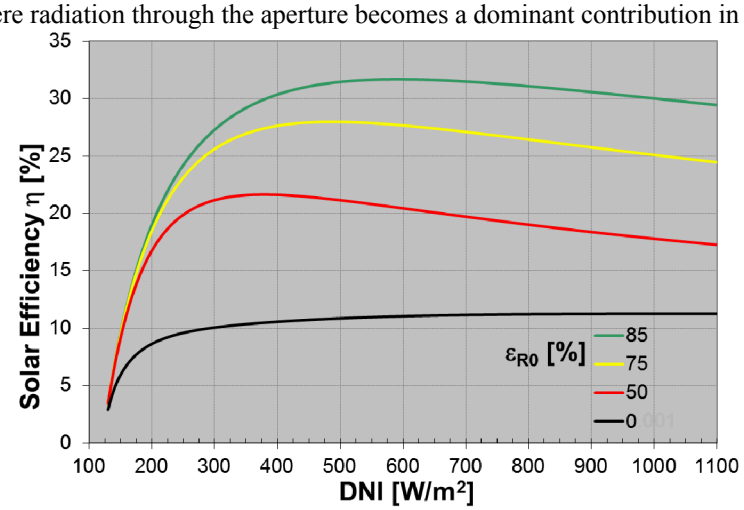

Figure 3. Fully converged calculation for η(DNI) away from the design point for several values of ε_{R0}.

The difference between the simple and complete model is especially apparent for DNI values between 200 W/m^2 and 700 W/m^2, and mid-range recuperator effectiveness values ($\varepsilon_{R0}\approx0.5$). The origin of this difference varies: In most of the the ε_{R0} range shown in Fig. 3 it is due to both effects explained above (ε_R increase and p_{TR}

decrease). However, for the limiting cases of ε_{R0}=0 and ε_{R0}=1 (latter not shown, as it is a practical impossibility), no ε_R gains are realized by decreasing flow. In these cases the entire difference in η(DNI) between the full model and simple model are entirely due to the effect of decreased p_{TR}. This is to some extent apparent for ε_{R0}=0.85 (Fig. 3), where only limited gains ε_R are available with DNI decrease, so η(DNI) decreases faster compared to mid-range values of ε_{R0}. For ε_{R0}=0, the nearly flat efficiency curve in the full model (as opposed to the simple model) is entirely due to $p_{TR}(DNI)<p_{TR,0}$.

These results elegantly demonstrate the operational flexibility of the particle reactor design, in addition to its design flexibility.[1] By adjusting only two operational parameters, namely oxide flow rate through the reactor (via the conveyor speed) and steam feed rate into the fuel production chamber, the reactor can be operated in a wide range of DNI with no loss of efficiency. There are, nonetheless, some limitations to these results that should be kept in mind. One is that, while efficiency increase with pressure decrease can be expected to be universal, the precise pressure dependence of this contribution is a function of the thermodynamic properties of the working oxide. Another limitation is in the assumed ideal behavior of the recuperator under decreased material flow. In practice, near unity recuperator effectiveness should not be expected at near zero flow.

Mindful of the latter limitation, we can still arrive to a good estimate of the annual average solar efficiency for a ceria-based cycle. We do this by conservatively assuming that efficiency is zero at some relatively high DNI value for which the recuperator behavior approximation is valid, and affords a margin of safety for other unanticipated non-ideal behavior. To do this, we observe that, irrespective of ε_{R0}, η(DNI)→0 for DNI≈125 W/m^2 – the point where radiation losses equal the solar flux at the aperture. We can therefore conservatively set DNI=300 W/m^2 as the value below which the reactor does not operate, constituting a roughly 2.5-factor margin of safety. Additionally, we set a wind speed limit of 25 mph, above which the reactor also does not operate. Under these limitations, and using typical meteorological year (TMY) hourly data for Dagget, CA [source], we calculate $\eta_{AA}(\varepsilon_{R0})$, and show the results in Fig. 4.

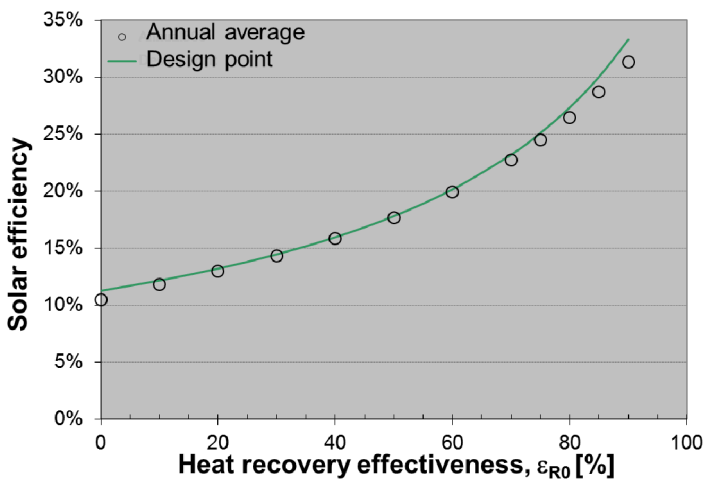

Figure 4. Annual average solar efficiency as function of recuperator effectiveness at the design point,$\eta_{AA}(\varepsilon_{R0})$. Open circles denote, η_{AA} whereas the solid line, included for comparison purposes, represents$\eta_0(\varepsilon_{R0})$.

The most striking result of these calculations is that in the majority of the ε_{R0} range under consideration there is little difference between η_0 and η_{AA}. In other words, the reactor can be operated with design-point efficiency throughout the entire year. This is especially true in the region of most interest – up to ε_{R0}≈0.75 – values that can reasonably expected to be achieved in practice, without requiring a prohibitively large recuperator. We note that the η_{AA}≈η_0 relationship also holds in the one case considered where only p_{TR}(DNI) plays a role, i.e. ε_{R0}=0.

In addition to the undiminished efficiency at low DNI, these results point to a possible solution to an issue that may decrease η_{AA} – overnight temperature decrease throughout the reactor. By a combination of good thermal insulation and heating the working oxide before DNI reaches 300 W/m^2 in the morning, this potential efficiency loss

may be partially or completely mitigated.

While the above efficiencies (both η and η_{AA}) are relatively high, they are still substantially lower than 100%. The majority of the losses take the form of waste heat, released as hot exhaust gasses leaving the fuel production chamber. In Fig. 5, we show the high quality (T≈1000°C) waste heat output as function of DNI. Note that this is after a portion of the heat had been subtracted to account for the heat equivalent of required mechanical work (primarily pumping). As expected, the amount of waste heat exceeds, sometimes considerably, the heat content of the produced H_2 fuel (286 kJ/mol) for virtually the entire operational range. Being of high quality, this heat can be used for balance of plant needs, including the relatively low need for water extraction from the atmosphere (only a few kJ/mol, conservatively) via, for example, a sorption mechanism. This is not to say that waste heat is a desirable reactor output, rather that there are substantial amounts of it. Waste heat decrease via efficiency improvements such as advanced reactive materials is anticipated and desirable, but it appears unrealistic that it can be reduced below the requirement for water extraction from the atmosphere for the running requirements of the reactor.

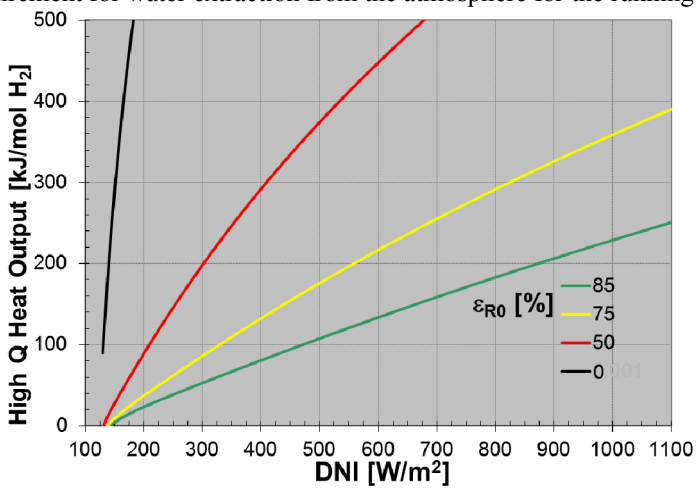

Figure 5. High quality waste heat output as function of DNI.

This result is of potentially far-reaching consequences, as the best solar locations are typically in deserts. A standalone facility that can fully function using only local resources (i.e. sunshine and air) obviates many of the objections to the technology based on the perception that vast amounts of scarce water would have to be purified and brought to desert areas from distant sources in order to produce meaningful quantities of fuel. The potential for locally producing feedstock water also highlights the advantage of high-temperature, two-step solar-thermochemical cycles over low temperature processes (e.g. photoelectrochemical), where feedstock water (to say nothing of other balance of plant needs) must be produced using an additional source of energy, thereby reducing the overall plant efficiency.

3. Conclusions

Acknowledgements

This work was supported by the U.S. Department of Energy Fuel Cell Technologies Program via the Solar Thermochemical Hydrogen (STCH) directive. Sandia is a multiprogram laboratory operated by Sandia Corporation, a Lockheed Martin Company, for the United States Department of Energy's National Nuclear Security Administration under Contract DE-AC04-94AL85000.

References

[1] I. Ermanoski, N.P. Siegel, E.B. Stechel, A New Reactor Concept for Efficient Solar-Thermochemical Fuel Production, Journal of Solar Energy Engineering, 135 (2013) 031002-031001 - 031010.
[2] R.J. Panlener, R.N. Blumenthal, J.E. Garnier, A Thermodynamic Study of Nonstoichiometric Cerium Dioxide, Journal of Physics and Chemistry of Solids, 36 (1975) 1213-1222.
[3] M. Ricken, J. Nölting, I. Riess, Specific Heat and Phase Diagram of Nonstoichiometric Ceria (CeO_{2-x}), Journal of Solid State Chemistry, 54 (1984) 89-99.